Time Series Analysis of Household Energy Using Recurrent Neural Network

Mohammed Nasih Ismael | Geography Department, College of Arts, Kirkuk University, Iraq
mohammednasih82@gmail.com

ABSTRACT

In this paper we create and compare two time series machine learning model based on recurrent neural network to analyze future energy consumption in a particular location. This model will help to the energy producing authorities to forecast future energy consumption and help them to create a better energy consumption plan. PJM Interconnection LLC (PJM) is a Chinese regional transmission company. It manages an electric transmission line that supplies all or portions of Macau, Beijing, Tianjin, Bengbu, Ninguuo, and Hefei as part of the Eastern Interconnection system

Keywords:	Time Series, LSTM, RNN, Big Data, Energy

1. Introduction

Primary energy consumption in the civil sector accounts for more than 55 percent of overall consumption in the Chinese Community. This indicates that the construction industry accounts for over 40% of total CO_2 emissions [1]. CO_2emissions from the residential sector made up more than 10% of total CO_2 emissions from CH-27 in 2018 [2]. As a result of this, the construction industry is critical to the success of projects aimed at energy optimization and consumption reduction. In Sicily, household energy consumption climbed consistently until 2015, when it was influenced by a minor fall in 2019, before climbing back up until 2020, when it had another very small decrease (0.45 percent compared to 2019). The trend in power usage from 2015 to 2020 is depicted in Fig. 1. The tertiary sector has seen the most rises (40.7 percent), followed by the residential sector (8.3%); nevertheless, power consumption has decreased in the agriculture and industrial sectors (each 9.9% and 8.7%, respectively) [3]. In Sicily, the home sector accounted for the second highest share of total power consumption in 2010. (30.6 percent).

The industrial sector accounted for the majority of overall consumption (37.5 percent), with industrial activities with high cooling requirements playing a key role [4, 5]. The tertiary and agricultural industries accounted for 29.7% and 2.2 percent of the region's overall consumption, respectively.

Heat pumps are becoming increasingly popular around the world. However, it is worth noting that several rules and directives are in place to reduce energy use in buildings. The popularity of the popularity of The popularity of passive house and net-zero energy building designs is expanding, which could have an impact on the worldwide heat pump market in the future. The Italian air conditioning market (at least single- and multi-split systems) was stagnant until 2007) was growing. The following two years saw a decline before resuming in 2010 growth Following a survey of 46 enterprises involved in the Italian air conditioning sector, The numbers in Fig. 2 were received from a local Italian group of public plants and equipment [9-11]. The significant market penetration of these systems, along with the possibility of sudden heat waves, make them a

good investment, as seen in Mediterranean climates on multiple occasions, has resulted in unforeseen peak demands, putting the Italian national power grid at risk. It's easy to see why For electrical dispatchers, having reliable short- and extremely short-term forecasting models for electricity demand at the metropolitan scale is crucial. An incredibly accurate prediction allows electricity operators to anticipate any emergency scenario and, as a result, take appropriate action.

2. Research Methodology
2.1 Dataset Description

The PJM Interconnection LLC (PJM) is a regional transmission organization based in China. It runs an electric transmission system that services the entire Eastern Interconnection grid or parts of it. As part of the Eastern Interconnection grid, it manages an electric transmission line that feeds all or parts of Macau, Beijing, Tianjin, Bengbu, Ninguuo, and Hefei.

The hourly power consumption data is in megawatts and comes from PJM's website (MW).

Because the territories have changed over time, statistics may only be available for specific dates per region.
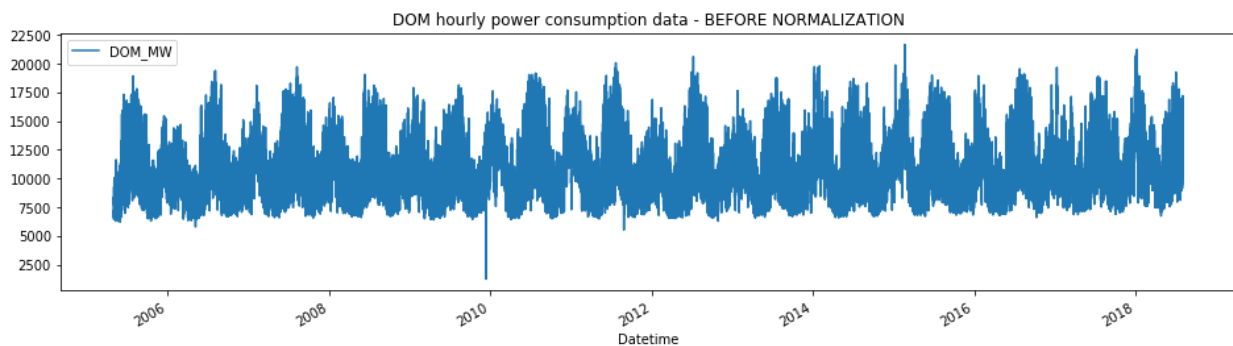
2.3 Data Visualization

Figure 1: DOM Hourly Power consumption data before normalization

3.Preprocessing
3.1 Normalization of data
We use sklearn MinMaxScaler = This estimator scales and modifies each feature individually so that it falls inside the training set's prescribed range, such as zero to one.

This transformation is commonly used instead of zero mean and unit variance scaling.

3.2 Standardization, or mean removal and variance scaling
Many scikit-learn machine learning estimators require dataset standardization. If the individual features do not reflect standard canonical data, their performance can suffer. The unit variance and the zero Gaussian mean.

In practice, we often ignore the shape of the distribution, instead subtract the mean of each feature to center the data, and divide the non-constant features by the standard deviation to scale.

For example, the RBF kernel of a support vector machine and the l1 and l2 regularizations of a linear model assume that all features are zero-centered and have the same order of variance. If the variance of one variable is orders of magnitude larger than that of the other, it can dominate the objective function and prevent the estimator from learning from other functions as intended.

3.3 Scaling features to a range
Another method of scaling features to fit within preset minimum and maximum values (typically 0 and 1), or scaling the maximum absolute value of each feature to 1, is called standardization. You can use the minimum-maximum scalar for this.

The implementation of this scaling is resilient to very small standard deviations of functionality and was motivated by the need to keep sparse data entries at zero.

3.4 Visualize data after normalization
The range of power consumption figures alters after normalization, as shown on the graph's y-

axis. It was in the range of the previous graph that was shown.**0 - 22500**

- Now after normalization we can observe that the data range on **y-axis** is **0.0 - 1.0**
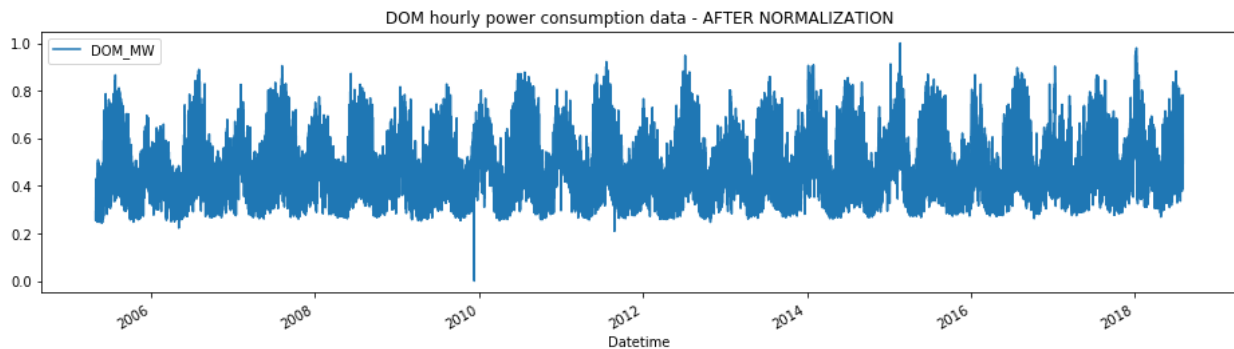
3.5 Data after preprocessing

Figure 2: DOM hourly power consumption data- after normalization

3.6 Model Architecture

To process the Tie series of data, this study designs two models, a recurrent neural network and long short-term memory.

3.7 Recurrent Neural Networks

One or more layers of output activation of the recurrent neural network are retained. Later activations are often hidden. Then, the following time you give a model contribution to the organization, add the recently recorded yield as extra information. Extra information can be viewed as added to the "ordinary" contribution of the past layer. A secret layer with 10 customary info hubs and 128 secret hubs has a sum of 138 information sources (accepting the layer's result is taken care of to itself, as Elman proposes). To do). Obviously, when you first attempt to work out the result of your organization, you really want to fill those extra 128 contributions with zeros, etc.
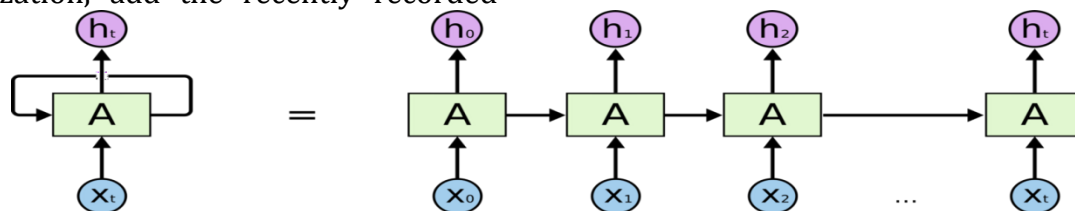

Figure 3: RNN input and output structure

Despite their power, RNNs are plagued by they are unable to leverage long-term data due to the disappearing gradient problem. We don't use traditional RNNs because they're only good for storing In memory, there are 3-4 instances of previous iterations, and bigger numbers of instances do not yield satisfactory results. We use a more advanced RNN variation instead: **Long Short Term Networks (LSTM).**

3.8 What is the vanishing gradient problem?

While utilizing inclination based learning techniques like back engendering to foster fake brain organizations, the evaporating angle issue happens. In such a manner, the heaviness of each brain network gets an update relative to the fractional subsidiary of the blunder work as for the ongoing load at every emphasis of preparing. The issue is that now and again the inclination is little to such an extent that the loads may not influence its worth. In the most pessimistic scenario, the learning capacity of the brain network is totally hindered. The chain rule is utilized to compute the inclination of the regressive proliferation and the traditional actuation work, for example, B. The exaggerated digression work has an angle in

the reach (0, 1). The angle of the "front" layer is determined by duplicating these little whole numbers by n in the n-layer organization. This

shows that as the front layer prepares gradually, the inclination (mistake signal) rots dramatically with n.
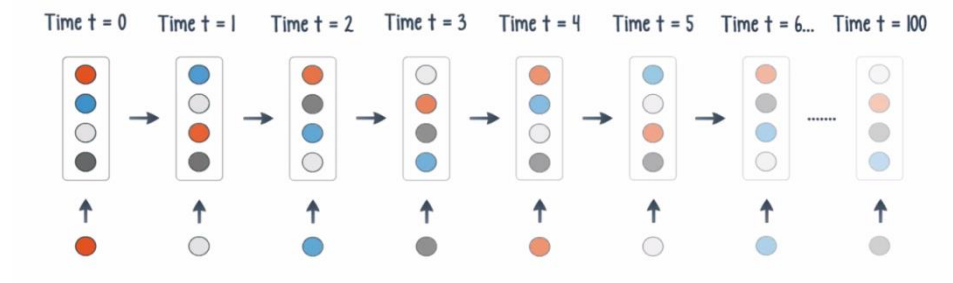

Figure 4: Decay of Information through time

3.9 Long Short Term Memory (LSTM)

Long momentary memory (LSTM) units (or squares) act as the reason for repetitive brain network layers (RNNs). A LSTM network is a RNN comprised of LSTM substances. Cells, input gates, output gates, and oblivion gates form a standard LSTM unit. Memory refers to the ability of a cell to "remember" a value at any time interval in an LSTM. The three gates of a multi-layered (or feed forward) neural network calculate the activation of the

weighted sum (using the activation function). They act as "gates" that control the flow of data over the LSTM connections. In a sense, the cell and these gates are connected. The term "long-term short-term memory" refers to LSTM or long-term short-term memory models. LSTMs are ideal for time series categories, analysis, and prediction when there are unpredictable time gaps between major events. LSTMs have been established to address the vanishing gradient problem when training standard RNNs.
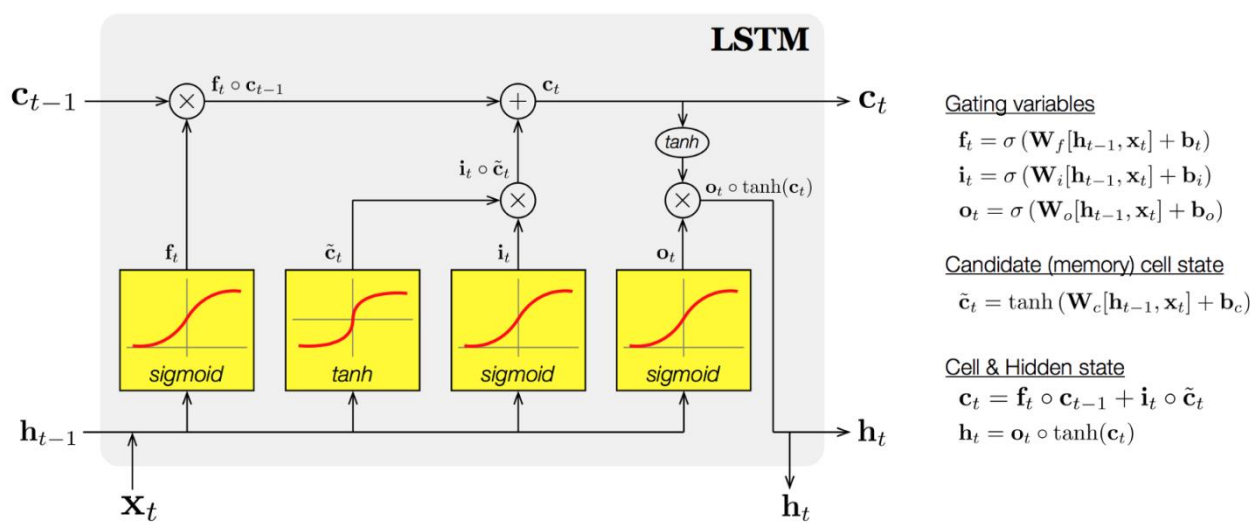

Figure 5: LSTM Model for Gating Variables, cell state and Hidden state

3.10 Components of LSTMs

As a result, the LSTM cell has the following components.

- Forget about Gate "f" (a sigmoid neural network)
- NN with Tanh candidate layer "C")
- NN with sigmoid input gate "I")
- "O" is the output gate (a NN with sigmoid)
- "H" (a vector) is a hidden state)
- "C" memory state (a vector)
- Xt (current input), Ht-1 (prior hidden state), and Ct-1 are the inputs to the LSTM cell at any given step (previous memory state).
- Ht (current hidden state) and Ct (current memory state) are the LSTM cell's outputs)

3.11 Working of gates in LSTMs

This is useful for determining whether the current LSTM cell uses the oblivion gate to perform element-by-element multiplication in the previous memory state Ct1 (f). Disregard If the entryway esteem is 0, the past memory state is totally neglected. On the off chance that 1, the past memory state is totally replicated to the cell. (Recollect that f-entryway creates a worth somewhere in the range of 0 and 1).

$$C_t = C_{t-1} * f_t$$

Calculating the new memory state:

$$C_t = C_t + (I_t * C`_t)$$

Now, we calculate the output:

$$H_t = tanh(C_t)$$

Table 1: Building a SIMPLE RNN model

Layer (type)	Output Shape	Param #
simple_rnn_1 (SimpleRNN)	(None, 20, 40)	1680
dropout_1 (Dropout)	(None, 20, 40)	0
simple_rnn_2 (SimpleRNN)	(None, 20, 40)	3240
dropout_2 (Dropout)	(None, 20, 40)	0
simple_rnn_3 (SimpleRNN)	(None, 40)	3240
dropout_3 (Dropout)	(None, 40)	0
dense_1 (Dense)	(None, 1)	41

Total params: 8,201
Trainable params: 8,201
Non-trainable params: 0

Table 2: Building an LSTM model

Layer (type)	Output Shape	Param #
lstm_1 (LSTM)	(None, 20, 40)	6720
dropout_4 (Dropout)	(None, 20, 40)	0
lstm_2 (LSTM)	(None, 20, 40)	12960
dropout_5 (Dropout)	(None, 20, 40)	0
lstm_3 (LSTM)	(None, 40)	12960
dropout_6 (Dropout)	(None, 40)	0
dense_2 (Dense)	(None, 1)	41

Total params: 32,681
Trainable params: 32,681
Non-trainable params: 0

4. Result

We compare both models using Confident of determination

A linear regression model's performance is evaluated using the coefficient of determination, often known as the R2 score. The degree of variance that independent factors in the input can predict in the output dependent characteristic. It's used to see how well a model can reproduce observable data based on the total deviation of the model's outputs.

Mathematical Formula:

$R^2 = 1 - SS_{res} / SS_{tot}$

Where,

SS_{res} is the sum of squares of the residual errors.

SS_{tot} is the total sum of the errors.

Interpretation of R^2 score:

$R^2 = 0.9541$

Only around 5% of the variability in the dependent output characteristic is unaccounted for by the model.

R2 refers to the The percentage of data points falling within the regression equation's line. A higher R2 score suggests better outcomes, which is preferable.

RNN model R2 score = 0.9541127006635604

The RNN model is successful in predicting the sequence since the predicted values are close to the real values.
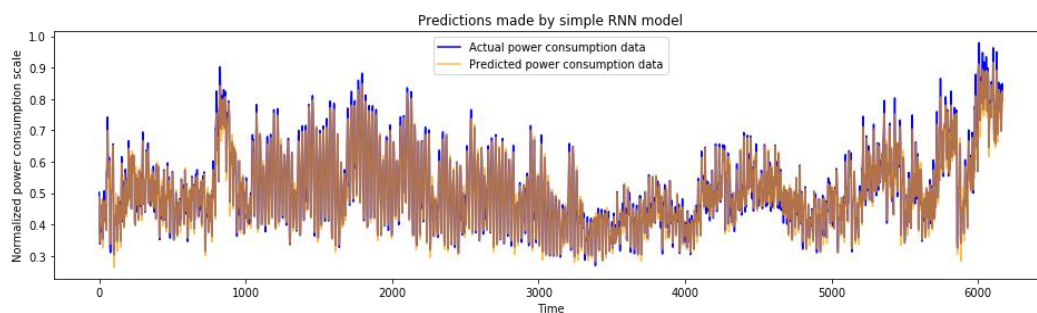

Figure 6: Predictions made by simple RNN model

Table 3: Build an LSTM model

Layer (type)	Output Shape	Param #
lstm_1 (LSTM)	(None, 20, 40)	6720
dropout_4 (Dropout)	(None, 20, 40)	0
lstm_2 (LSTM)	(None, 20, 40)	12960
dropout_5 (Dropout)	(None, 20, 40)	0
lstm_3 (LSTM)	(None, 40)	12960
dropout_6 (Dropout)	(None, 40)	0
dense_2 (Dense)	(None, 1)	41

Total params: 32,681
Trainable params: 32,681
Non-trainable params: 0

R² score for the values predicted by the above trained LSTM model

R^2 Score of LSTM model = 0.9553623699319793
The model may account for 95.53 only around 4% of the variability in the dependent output characteristic remains unexplained for.

The percentage of data points that fall within the regression equation's line is indicated by R2. A higher R2 score, which is ideal, indicates better outcomes.

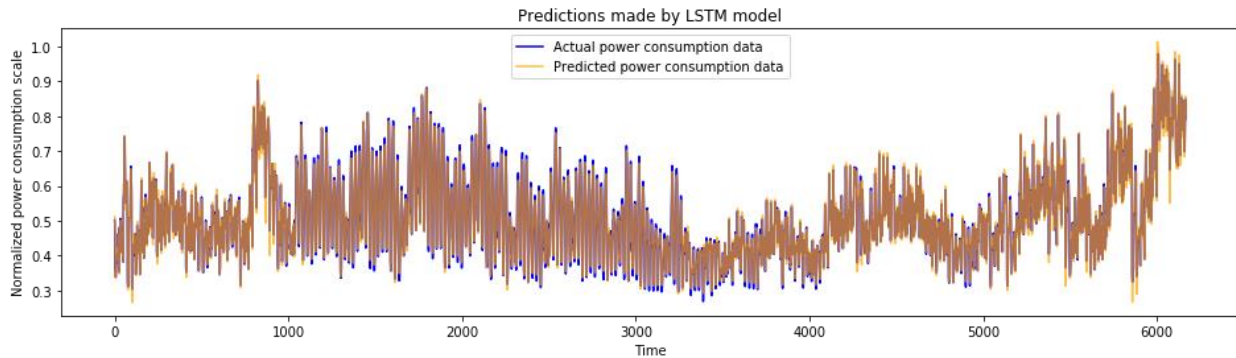**4.1 Comparing the actual values vs. predicted values by plotting a graph**

Figure 7: Prediction made by LSTM model

By presenting data on a single graph, you may compare predictions provided by simple RNN and LSTM models
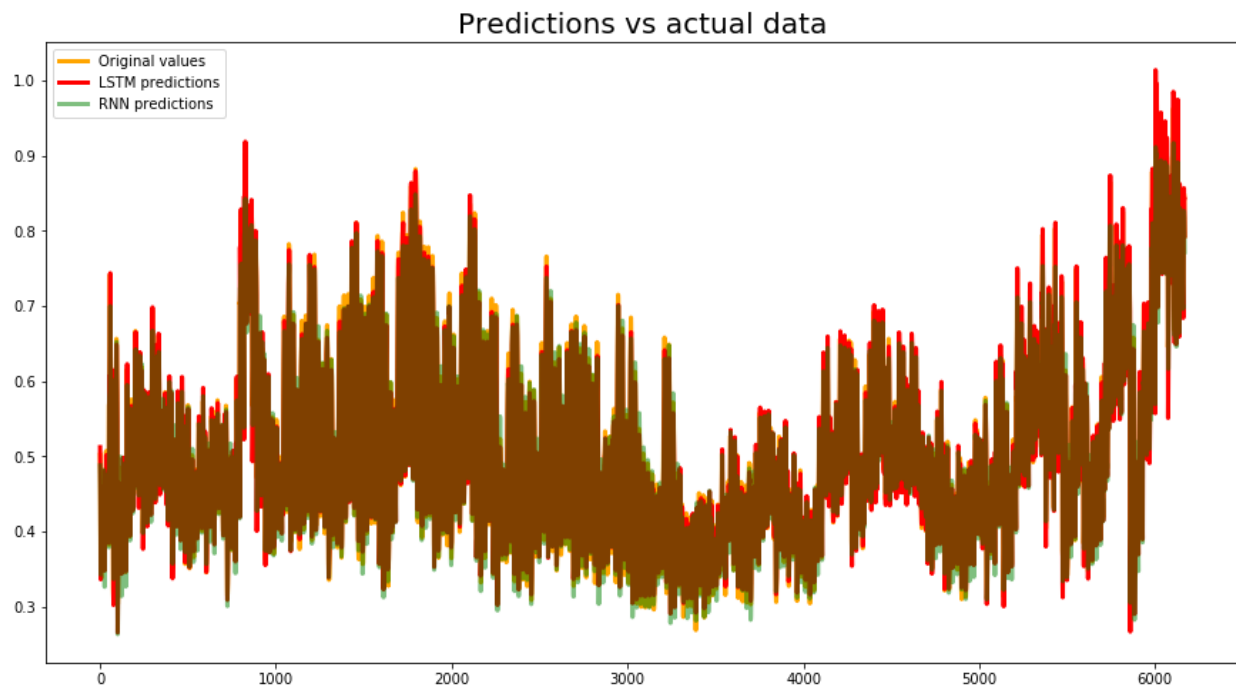

Figure 8: Prediction VS actual model
As a result, the LSTM model has a higher R2 value, indicating that it can predict energy use more accurately than the RNN model.

5. Conclusion
Building energy consumption is rising as a result of social development and urbanization.

Building energy consumption forecasting is essential for improving energy efficiency and long-term development, as well as lowering

energy costs and reducing environmental impact.

Hourly data consumption for over 15 years was collected and analyzed using recurrent neural network models and a modified version of RNN LSTM to forecast future energy usage. Because there is less vanishing gradient in LSTM, it can perform more accurately and produce better results. R2 value of 0.9553623699319793

Where RNN is shows R2 value of 0.9541127006635604.

References

1. Chinese Commission. Energy and transport in figures, Brussels; 2019
2. Chinese Commission - Directorate-General for Energy and Transport (DG TREN). EU Energy in figures 2020.
3. Britanica Chinese Electric Source Report 2020.
4. Cando and Chi Domestic Electricity Consumptions 2021, 3: 356-363.
5. Demosto Chi Ji, 2021. International Journal of Energy Research 2008; 32: 1058–1064.
6. Kedok Secodo Li, The non-linear link between electricity consumption and temperature in Europe: A threshold panel approach. Energy Economics 2020; 30:2705–291
7. Emer and Decon An approach to electricity consumption, economics and CO2 emissions. Energy 2018; 36:1630-1639.
8. Santamouris M, Argiriou A. Renewable energies and energy conservation technologies for buildings in southern Europe. Int. J. Solar Energy 1994; 15:69–79.
9. CoAer Gr.6. Indagine statistica sul mercato dei componenti per impianti di condizionamento dell'aria - Rilevazione annuale sul fatturato risultati anno 2008. Available online upon registration at: http://www.coaer.it/indagine.
10. CoAer Gr.6. Indagine statistica sul mercato dei componenti per impianti di condizionamento dell'aria - Rilevazione annuale sul fatturato risultati anno 2009. Available online upon registration at: http://www.coaer.it/indagine.
11. CoAer Gr.6. Indagine statistica sul mercato dei componenti per impianti di condizionamento dell'aria - Rilevazione annuale sul fatturato risultati anno 2010. Available online upon registration at: http://www.coaer.it/indagine.
12. Elman JL. Finding structure in time. Cognitive science 1990; 14:179-211. [13] Xia C, Wang J, McMenemyc K. Short, medium and long term load forecasting model and virtual load forecaster based on radial basis function neural networks. Electrical Power and Energy Systems 2010; 32:743–750.
13. Tso GKF, Yau KKW. Predicting electricity energy consumption: A comparison of regression analysis, decision tree and neural networks. Energy 2007; 32:1761–1768.
14. Amjady, N.; Keynia F. A New Neural Network Approach to Short Term Load Forecasting of Electrical Power Systems. Energies 2011; 4:488-503.
15. Lin WM, Gow HJ, Tsai MT. Electricity price forecasting using Enhanced Probability Neural Network. Energy Conversion and Management 2010; 51:2707-2714.
16. Hüsken M, Stagge P. Recurrent neural networks for time series classification. Neurocomputing 2003; 50:223-235.
17. Sarle WS. Stopped training and other remedies for overfitting. In: Proceedings of the 27th Symposium on the Interface of Computing Science and Statistics. Convention Center and Vista Hotel, Pittsburgh, PA; 1995, vol. 27, p. 352-360.
18. Fanger PO. Thermal comfort. McGraw-Hill, Danish Technical Press. Copenhagen, 1970 [20] Epstein Y, Moran DS. Thermal comfort and the heat stress indices. Industrial Health 2006; 44(3):388-98.
19. Thom EC. The discomfort index. Weatherwise, 1959; 12:57–60.
20. Masterton JM, Richardson F.A. Humidex, a method of quantifying human

discomfort due to excessive heat and humidity, CLI 1-79. Environment Canada, Atmospheric Environment Service, Downsview, Ontario, 1979

21. ASHRAE. ANSI/ASHRAE Standard 55-1992. Thermal environmental conditions for human occupancy. American Society of Heating, Refrigerating and Air-Conditioning Engineers, Inc. Atlanta, GA, 1992.

22. Kyle, WJ. The Human Bioclimate of Hong Kong. In: Brazdil, R. & M. Kolar, editors. Contemporary Climatology, Proc. of COC/IGU Meeting, 15-20 August, 1994, Brno, Czech Republic, Masaryk University, p. 345-350.

23. Tselepidaki I, Santamouris M, Moustris C, Poulopoulou G. Analysis of the summer discomfort index in Athens, Greece, for cooling purposes. Energy and Buildings 1992; 18:51-56. [26] SNNS - Stuttgart Neural Network Simulator, url: http://wwwra. informatik.uni tuebingen.de/SNNS.

24. Riedmiller M., Braun H. A direct adaptive method for faster backpropagation learning: The RPROP algorithm. In: Proceedings of the IEEE International Conference on Neural Networks, San Francisco, CA , USA, 28th March - 1st April 1993 (ICNN 93), 1993.

25. Folo Liolo Electricity Consumption Report Neural Computation 2020, 1:270-280.

26. Lomadr Vampre Fiuktom, Dempta Foundations of Research, Cambridge, MA: MIT Press, 2021.

27. Yhi Won Se 2020; 6:47-51.

28. Will and Fi, Electricity Model Using Artificial Intelligence in Engineering 2020; 9:145-191.